Available online at www.sciencedirect.com
SCIENCE DIRECT®
Journal of Magnetic Resonance 177 (2005) 56–66
JMR Journal of Magnetic Resonance
www.elsevier.com/locate/jmr

Solid state ^{31}P and ^{207}Pb MAS NMR studies on polycrystalline *O*,*O*′-dialkyldithiophosphate lead(II) complexes

Anna-Carin Larsson [a], Alexander V. Ivanov [b], Kevin J. Pike [c], Willis Forsling [a], Oleg N. Antzutkin [a,*]

[a] *Division of Chemistry, Luleå University of Technology, S-971 87 Luleå, Sweden*
[b] *Amur Integrated Research Institute, Far Eastern Branch of the Russian Academy of Sciences, 675000, Blagoveschensk, Amur Region, Russia*
[c] *Materials and Engineering Science, ANSTO, Lucas Heights, NSW 2234, Australia*

Received 24 February 2005; revised 30 June 2005
Available online 15 August 2005

Abstract

A number of lead(II) *O*,*O*′-dialkyldithiophosphate complexes were studied by ^{13}C, ^{31}P, and ^{207}Pb MAS NMR. Simulations of ^{31}P chemical shift anisotropy using spinning sideband analysis reveal a linear relationship between the S—P—S bond angle and the principal values δ_{22} and δ_{33} of the ^{31}P chemical shift tensor. The ^{31}P CSA data were used to assign ligands with different structural functions. In the cases of diethyldithiophosphate and di-*iso*-butyldithiophosphate lead(II) complexes, $^{2}J(^{31}\text{P}, ^{207}\text{Pb})$-couplings were resolved and used to confirm the suggested assignment of the ligands. The SIMPSON computer program was used to calculate ^{31}P and ^{207}Pb spectral sideband patterns.

Keywords: ^{31}P CP/MAS; ^{207}Pb MAS NMR; ^{31}P chemical shift anisotropy; ^{207}Pb chemical shift anisotropy; *O*,*O*′-dialkyldithiophosphate lead(II) complexes; $^{2}J(^{31}\text{P},^{207}\text{Pb})$-coupling

1. Introduction

Dialkyldithiophosphates (dtp) are widely used as collectors in the selective froth flotation of sulfide minerals and as analytical reagents for extraction and spectrophotometric determination of metal ions [1]. Over the years various *O*,*O*′-dialkyldithiophosphate metal complexes have been investigated by single-crystal X-ray diffraction (e.g., [2–11] and references therein). The dithiophosphate ligands can adopt different structural functions: terminal, bridging or combined, (tridentate), which leads to a variety of structures of dtp compound, i.e., mono-, bi- or polynuclear metal complexes [2–11]. Recently, we have reported on a correlation between the ^{31}P chemical shift tensor (CST) principal values and the type of dtp ligands in different nickel(II) and zinc(II) dtp complexes [12] found using spinning sideband analysis on ^{31}P CP/MAS NMR spectra. These correlations have been further confirmed by quantum mechanical ab initio calculations [12]. It has been revealed that the principal value δ_{22}, but not δ_{11} and δ_{33}, of the ^{31}P chemical shift tensor is very sensitive to the S—P—S bond angle: δ_{22} increases substantially with an increase in the S—P—S bond angle, while both δ_{11} and δ_{33} are almost constant. Generally, the terminal ligands in nickel(II) and zinc(II) dtp complexes have smaller S—P—S angles (95°–97°), and the phosphorus sites in these ligands have values for $\delta_{22} \approx 69$–78 ppm, while the larger S—P—S angles (97°–105°) in the bridging ligands correspond to $\delta_{22}(^{31}\text{P}) \approx 94$–$124$ ppm. These results can be used for determining the type of surface coordination and geometry of dialkyldithiophosphate ligands chemisorbed on mineral surfaces, and for a better understanding of the mechanisms in froth flotation of sulfide ores.

* Corresponding author. Fax: +46 920 491199.
E-mail address: Oleg.Antzutkin@ltu.se (O.N. Antzutkin).

1090-7807/$ - see front matter © 2005 Elsevier Inc. All rights reserved.
doi:10.1016/j.jmr.2005.07.007

In this study, we measure the ^{31}P chemical shift anisotropy of different *O*,*O*′-dialkyldithiophosphate lead(II) complexes and investigate further the correlations between these data and the structural parameters of the $[O_2PS_2]^-$-moiety, i.e., P—O, and P—S bond lengths and O—P—O and S—P—S bond angles. The ^{31}P CSA analysis, based on a Mathematica program developed by Levitt and co-workers [13], was performed by evaluating the integrals of the spinning sidebands in the CP/MAS NMR spectra obtained at moderate and slow sample spinning (2–5 kHz). For diethyldithiophosphate and di-*iso*-butyldithiophosphate lead(II) complexes, two-bond *J*-couplings between ^{31}P and ^{207}Pb ($I = 1/2$) nuclei were resolved in the ^{31}P CP/MAS NMR spectra and were also used in the assignment of the ligands. In addition, ^{207}Pb MAS NMR spectra of three lead(II) dtp complexes are also presented.

The SIMPSON [14] computer program was used to calculate the MAS NMR spectra of the ^{31}P to provide direct comparisons with the experiments, and of the ^{207}Pb to estimate the CSA parameters for the three lead(II) dtp complexes.

The crystal structures of a few Pb(II) dtp compounds have been determined previously: (i) the diethyldithiophosphate lead(II) complex, $[Pb\{S_2P(OC_2H_5)_2\}_2]$ [7], consists of mononuclear units with two terminally coordinated ligands (see Fig. 1A). The ligands are connected to the neighboring monomeric units through weak S—O′ and S—Pb′ bonds, forming a polymeric structure. (ii) The di-*iso*-butyldithiophosphate lead(II) complex, $[Pb_2\{S_2P(O\text{-}i\text{-}C_4H_9)_2\}_4]$ [8], is a dimeric unit, including pairs of ligands with terminally chelating or tridentate structural functions (see Fig. 1B). (iii) The di-*iso*-propyl- [9,10], (iv) dipropyl- [11], and (v) di-*cyclo*-hexyldithiophosphate [11] lead(II) complexes consist of polymeric chains, $[Pb\{S_2P(OR)_2\}_2]_n$ ($R = i\text{-}C_3H_7$, C_3H_7, $c\text{-}C_6H_{11}$), in which the ligands display only tridentate structural functions (see Fig. 1C).

Table 1 shows the most important crystallographic data of the lead(II) dtp complexes presented in this study.

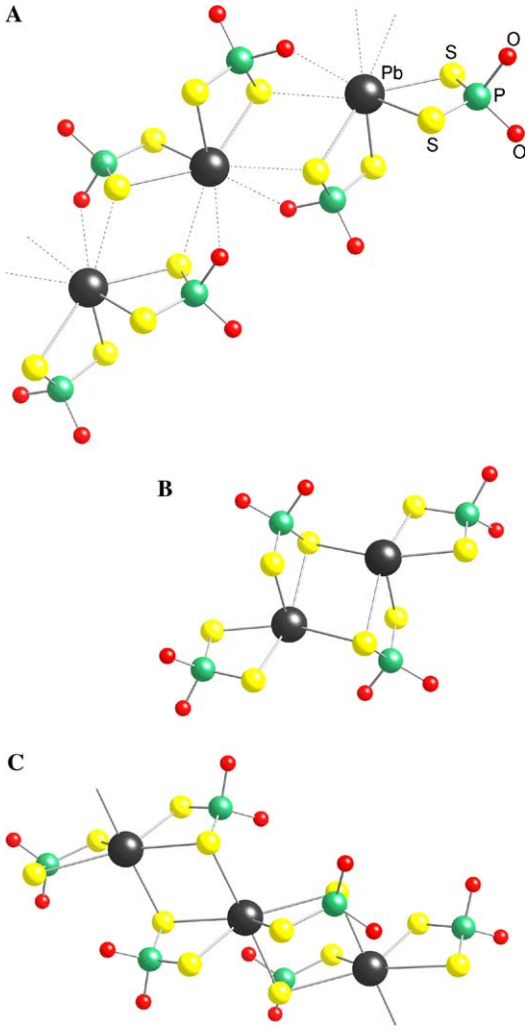

Fig. 1. Molecular structures of monomeric lead(II) diethyl- (A), dimeric di-*iso*-butyl- (B) and polymeric di-*iso*-propyl- (C) dithiophosphate complexes.

2. Experimental

2.1. Materials

Eight polycrystalline potassium *O*,*O*′-dialkyldithiophosphates, $K\{S_2P(OR)_2\}$ ($R = C_2H_5$, C_3H_7, $i\text{-}C_3H_7$, C_4H_9, $i\text{-}C_4H_9$, $s\text{-}C_4H_9$, $i\text{-}C_5H_{11}$, $c\text{-}C_6H_{11}$), which are the components of the commercial collectors Danafloats, were provided to us by 'CHEMINOVA AGRO A/S'. *O*,*O*′-dialkyldithiophosphate lead(II) complexes **1**–**8** (see Table 2) were prepared by mixing aqueous solutions of $Pb(NO_3)_2$ ('Merck') and corresponding potassium *O*,*O*′-dialkyldithiophosphates. Precipitated complexes were filtered off, washed with water, dried naturally, and recrystallized from organic solvents. The potassium dialkyldithiophosphate salts, as well as two of the lead(II) dialkyldithiophosphate complexes, have been previously characterized by solid state ^{13}C CP/MAS NMR [4,11]. ^{13}C chemical shifts of the solid lead(II) dtp complexes and potassium dtp salts are given below (δ, ppm):

$[Pb\{S_2P(OC_2H_5)_2\}_2]$ (**1**): 1:1—65.4, 63.8, 62.1 (2:1:1, —OCH_2—), 18.2, 17.7, 17.3, 16.6 (1:1:1:1, —CH_3). Cf. data for the initial $K\{S_2P(OC_2H_5)_2\}$: (1:1)—63.2 (—OCH_2—), 18.1, 18.0 (1:1, —CH_3).

$[Pb\{S_2P(OC_3H_7)_2\}_2]_n$ (**2**): (1:1:1)—71.1, 70.4, 69.4, 69.0 (1:1:1:1, —OCH_2—), 24.8, 24.5 (1:1, —CH_2—), 10.7, 10.6, 10.5 (1:3:2, —CH_3). Cf. data for the initial $K\{S_2P(OC_3H_7)_2\}$: (1:1:1)—71.7, 68.9, 68.8 (2:1:1, —OCH_2—), 25.0, 24.1 (1:1, —CH_2—), 10.2, 9.9, 8.9 (1:2:1, —CH_3).

$[Pb\{S_2P(O\text{-}i\text{-}C_3H_7)_2\}_2]_n$ (**3**): (1:2)—75.4, 74.4, 71.9 (2:3:3, —OCH=), 26.1, 25.9, 25.2, 24.7, 24.5, 24.2, 23.9 (2:2:5:3:1:2:1, —CH_3). Cf. data for the initial

Table 1
Crystal data for dialkyldithiophosphate lead(II) complexes

Complex	P—S (Å)	S—P—S (°)	P—O (Å)	O—P—O (°)	S—Pb (Å)[a]	O—Pb′ (Å)
$[Pb\{S_2P(OC_2H_5)_2\}_2]$ [7]	1.995	115.4	1.59	100.1	2.75 T	3.04
	1.969		1.62		3.00 T	
					3.47 B	
	1.991	116.2	1.61	105.2	2.79 T	3.00
	1.968		1.59		3.02 T	
					3.48 B	
$[Pb\{S_2P(OC_3H_7)_2\}_2]_n$ [11]	1.974	116.16	1.584	105.1	3.21 T	3.05
	1.984		1.594		2.84 T	
	1.977				2.93 B	
	1.996	114.91	1.581	100.7	2.80 T	3.43
			1.576		3.14 T	
					3.12 B	
$[Pb\{S_2P(O^iC_3H_7)_2\}_2]_n$ [9,10]	2.000	113.8	1.584	110.5	3.23 T	3.43
	1.982		1.582		2.76 T	
	1.958					
	1.944	114.6	1.556	100.7	2.98 B	3.56
			1.584		2.77 T	
					3.18 T	
					3.03 B	
$[Pb_2\{S_2P(O^iC_4H_9)_2\}_4]$ [8]	1.994	113.9	1.55	100.4	2.76 T	3.48
	1.951		1.60		3.13 T	
	1.985		1.57		3.44 B	
	1.986	112.0	1.56	97.3	2.76 T	
					2.77 T	
$[Pb\{S_2P(O^cC_6H_{11})_2\}_2]_n$ [11]	1.994	114.35	1.580	101.0	2.86 T	3.80
	1.994		1.588		3.33 T	
	1.979		1.580		2.93 B	
	2.005	114.14	1.590	100.5	3.10 T	3.26
					2.75 T	
					3.20 B	

[a] T, terminal distance (Pb—S); B, bridging distance (Pb′—S).

Table 2
^{31}P chemical shift data for lead dithiophosphate compounds. 95.4% joint confidence limit

Complex	δ_{iso} (ppm)	J (Hz)	δ_{aniso} (ppm)	η	δ_{11} (ppm)	δ_{22} (ppm)	δ_{33} (ppm)
$[Pb\{S_2P(OC_2H_5)_2\}_2]$	98.5 ± 0.1	83	−76.4 ± 1.2	0.38 ± 0.06	151 ± 2	122 ± 5	22.1 ± 1.2
	97.2 ± 0.1	79	−66.0 ± 1.3	0.69 ± 0.05	153.0 ± 2.0	107 ± 4	31.2 ± 1.3
$[Pb\{S_2P(OC_3H_7)_2\}_2]_n$	98.1 ± 0.1		−66.6 ± 0.9	0.64 ± 0.04	152.8 ± 1.4	110 ± 3	31.6 ± 1.0
	97.3 ± 0.1		−78.6 ± 0.9	0.22 ± 0.05	145 ± 2	128 ± 5	18.7 ± 0.9
$[Pb\{S_2P(O\text{-}i\text{-}C_3H_7)_2\}_2]_n$	96.5 ± 0.2		−60.1 ± 1.3	0.83 ± 0.05	151.6 ± 1.8	102 ± 4	36.4 ± 1.4
	96.2 ± 0.2		−57.7 ± 1.0	0.86 ± 0.04	149.7 ± 1.5	100 ± 3	38.4 ± 1.0
$[Pb\{S_2P(OC_4H_9)_2\}_2]_n$	100.0 ± 0.2		−69.3 ± 1.9	0.60 ± 0.07	156 ± 3	114 ± 6	30.7 ± 1.9
	98.2 ± 0.2		−81.8 ± 1.5	0.22 ± 0.10	148 ± 4	130 ± 9	16.4 ± 1.6
$[Pb_2\{S_2P(O\text{-}i\text{-}C_4H_9)_2\}_4]$	98.1 ± 0.2	309;57	−63.1 ± 1.0	0.91 ± 0.03	158.5 ± 1.4	101 ± 3	35.0 ± 1.0
	94.5 ± 0.1	140	61.3 ± 0.8	0.38 ± 0.05	155.8 ± 0.8	76 ± 3	52.1 ± 1.5
$[Pb\{S_2P(O\text{-}s\text{-}C_4H_9)_2\}_2]_n$[a]	94.4 ± 1.1						
$[Pb\{S_2P(O\text{-}i\text{-}C_5H_{11})_2\}_2]_n$	99.0 ± 0.1		−69.4 ± 1.1	0.59 ± 0.05	154.1 ± 1.9	113 ± 4	29.7 ± 1.1
	98.7 ± 0.1		−68.8 ± 1.2	0.65 ± 0.05	155.4 ± 1.8	111 ± 4	29.9 ± 1.2
$[Pb\{S_2P(O\text{-}c\text{-}C_6H_{11})_2\}_2]_n$	99.6 ± 0.2		−59.0 ± 1.1	0.83 ± 0.05	153.5 ± 1.7	105 ± 3	40.7 ± 1.1
	95.6 ± 0.2		−64.4 ± 1.2	0.88 ± 0.04	156.1 ± 1.7	100 ± 3	31.2 ± 1.2

[a] Too broad signal to make unambigious simulations of ^{31}P CSA parameters.

$K\{S_2P(O\text{-}i\text{-}C_3H_7)_2\}$: (1:2)—73.0, 72.8, 70.5, 69.9 (1:1:1:1, —OCH═), 27.0, 26.7, 26.3, 25.4, 25.0, 24.1 (1:1:2:6:2:4, $—CH_3$).

$[Pb\{S_2P(OC_4H_9)_2\}_2]$ (the molecular structure is not reported) (**4**): 1:1:1:1—69.2, 67.9, 67.5 (1:1:2, $—OCH_2—$), 33.5, 33.1 (5:3, $—CH_2—$), 20.1, 19.5 (1:3, $—CH_2—$), 16.2, 15.2, 14.9, 14.7 (1:1:1:1, $—CH_3$). Cf. data for the initial $K\{S_2P(OC_4H_9)_2\}$: (1:1:1:1)—70.3, 67.9 (1:1, $—OCH_2—$), 34.9, 31.7, 31.5 (2:1:1, $—CH_2—$), 19.7, 19.3 (1:1, $—CH_2—$), 14.8, 14.4, 14.0, 13.5 (1:1:1:1, $—CH_3$).

[$Pb_2\{S_2P(O\text{-}i\text{-}C_4H_9)_2\}_4$] (**5**): (1:1:2)—75.1, 73.8, 73.2, 72.8 (1:1:1:1, —OCH_2—), 29.9, 29.8, 29.6, 29.5 (1:1:1:1, —CH=), 20.7, 20.1, 19.9, 19.8 (1:3:3:1, —CH_3). Cf. data for the initial $K\{S_2P(O\text{-}i\text{-}C_4H_9)_2\}$: (1:1:2)—75.1, 74.2, 73.5, 73.2, 72.9 (—OCH_2—), 29.9, 29.8, 29.7 (—CH=), 21.1, 21.0, 20.9, 20.8, 20.7, 20.6, 20.4, 20.3, 20.2, 20.1 (—CH_3).

[$Pb\{S_2P(O\text{-}s\text{-}C_4H_9)_2\}_2$] (the molecular structure is not reported) (**6**): (1:1:1:1)—77.1 (OCH—), 31.3, 30.9 (1:1, —CH_2—), 22.1, 21.6, 21.2, 20.9 (1:9:4:2, —CH_3), 10.1, 9.7 (3:1, —CH_3). Cf. data for the initial $K\{S_2P(O\text{-}s\text{-}C_4H_9)_2\}$: (1:1:1:1)—77.5 (OCH—), 31.7, 31.5, 31.1 (—CH_2—), 22.0, 21.2 (—CH_3), 12.0 (—CH_3).

[$Pb\{S_2P(O\text{-}i\text{-}C_5H_{11})_2\}_2$] (the molecular structure is not reported) (**7**): (1:1:3)—67.0, 65.2 (3:1, —OCH_2—), 40.0, 39.6 (1:1, —CH_2—), 26.2, 25.8, 24.7, 24.3, 24.2, 24.0, 23.8, 22.7, (—CH_3). Cf. data for the initial $K\{S_2P(O\text{-}i\text{-}C_5H_{11})_2\}$: (1:1:1:2)—66.6 (—$OCH_2$—), 41.0, 39.1 (1:1, —$CH_2$—), 26.7, 26.4, (1:1, —CH=), 25.0, 23.9, 23.6, 22.9, 22.7 (—CH_3).

$[Pb\{S_2P(O\text{-}c\text{-}C_6H_{11})_2\}_2]_n$ (**8**): (1:2:3)—78.8, 76.0, 74.2 (2:1:1, —OCH=), 35.5, 34.3, 31.9 (2:1:1, *o*-CH_2—), 26.2, 25.5, 21.9 (3:2:1, *m*-, *p*-CH_2—). Cf. data for the initial $K\{S_2P(O\text{-}c\text{-}C_6H_{11})_2\}$: (1:2:3)—79.9, 78.8, 78.1, 77.1 (1:1:1:1, —OCH=), 35.7, 35.2, 34.7, 33.9 (*o*-CH_2—), 26.2 (*m*-, *p*-CH_2—).

2.2. NMR measurements

Solid-state ^{31}P magic-angle-spinning (MAS) NMR spectra were recorded on a Varian/Chemagnetics Infinity CMX-360 ($B_0 = 8.46$ T) spectrometer using cross-polarization (CP) from the protons together with proton decoupling [15]. The ^{31}P operating frequency was 145.73 MHz. The proton $\pi/2$ pulse duration was 5.0 μs, CP mixing times varied between 3 and 5 ms for different samples and the nutation frequency of protons during decoupling was $\omega_{nut}/2\pi = 64$ kHz. The acquisition length was 4096 and the spectrum width was 50 kHz. From 4 to 32 transients spaced by a relaxation delay of 5 s were accumulated. Powder samples were packed in zirconium dioxide standard double bearing 7.5 mm rotors. Spectra of all samples were recorded at two or more different spinning frequencies, between 2 and 5 kHz, and their isotropic chemical shift data (in the deshielding, δ-scale) are given with respect to 85% H_3PO_4 [16] (here 0 ppm, externally referenced), which was mounted in a short 5 mm glass tube and placed in a 7.5 mm rotor to avoid errors due to differences in the magnetic susceptibility.

Solid-state ^{13}C CP/MAS NMR spectra for all samples were recorded with an operating frequency of at 90.52 MHz. The proton $\pi/2$ pulse duration was 4.5 μs, CP mixing time 2 ms and the nutation frequency of protons during both cross-polarization and decoupling was $\omega_{nut}/2\pi = 58$ kHz. From 664 to 1644 transients spaced by a relaxation delay of 2 s were accumulated. The isotropic chemical shifts are referenced to the least shielded resonance of solid adamantane at 38.56 ppm relative to TMS [17].

Solid-state ^{207}Pb MAS NMR spectra were recorded with a single-20° pulse experiment with proton decoupling. The ^{207}Pb operating frequency was 75.28 MHz. The acquisition length was 8192 and the spectrum width was 1000 kHz. Powder samples were packed in zirconium dioxide standard double bearing 4 mm rotors. Ca. 10,000–20,000 transients spaced by a relaxation delay of 8 s were accumulated. Two different spinning frequencies (11.3 and 12 kHz) were used and the isotropic chemical shifts are given with respect to $Pb(NO_3)_2$, externally referenced, and temperature calibrated: $\delta_{iso} = -3492.5$ ppm, ($T = 292$ K) [18].

^{207}Pb CP/MAS experiments were not successful on these compounds as the distance between ^{207}Pb and protons is long and the $T_{1\rho}$ relaxation time is probably short. In addition, problems with ringing from the probe made the initial part of the FID signal heavily distorted. The attempt to avoid the latter problem by using a rotor-synchronized echo experiment under MAS was unsuccessful due to large distortions in the line shape: (i) the large anisotropy of the lead sites makes the direct excitation of the spectral edges insufficient, (ii) relaxation of the signal to thermal equilibrium occurs faster at the edges than in the central region of the spectrum, near the carrier frequency. 180° echo pulses aggravate the problems since the pulse delay must be chosen to be unreasonably long to avoid saturation of the NMR signal. To avoid all these problems a single-pulse experiment with proton decoupling was performed and a 20° pulse (0.45 μs) was used instead of a 90°-pulse, to shorten the experimental time. To decrease the distortions of the lineshape caused by acoustic ringing of the probe, the first 40 data points in the FID were deleted, and 44 (40 + 4 for the acquisition and receiver delays, totalling 45 μs) zero points were then added at the beginning of the FID to avoid phasing problems in the spectra. This procedure had only minor effects on the spectral line intensities because the FID of the samples under study last for ~1.3 ms.

2.3. CSA simulations

Simulations of the ^{31}P chemical shift anisotropies were performed in a Mathematica-based program developed by Levitt and co-workers [13]. The input file to the Mathematica program consists of the experimental sideband intensities, the experimental spinning frequency, the Larmor frequency and the experimental noise variance. The program plots the χ^2 statistics as a function of the two chemical shift anisotropy parameters δ_{aniso} and η, with a minimum at certain values of δ_{aniso} and η. The joint confidence limits of the two CSA parame-

ters are bound by the contours $\chi^2 = \chi^2_{\min} + 2.3$ (68.3% confidence limit) and $\chi^2 = \chi^2_{\min} + 6.17$ (95.4% confidence limit) [19].

The principal values of the tensor can thus be recalculated from the two parameters δ_{aniso} and η and the isotropic chemical shift:

$$\delta_{\text{iso}} = \frac{\delta_{xx} + \delta_{yy} + \delta_{zz}}{3},$$
$$\delta_{\text{aniso}} = \delta_{zz} - \delta_{\text{iso}},$$
$$\eta = \frac{\delta_{yy} - \delta_{xx}}{\delta_{\text{aniso}}}.$$

The sideband intensities were measured with the deconvolution method using the Varian 'Spinsight' spectrometer software. Values of δ_{aniso} and η from ^{31}P simulations at two different spinning frequencies were obtained and their mean and the mean error were calculated using the following equations:

$$\langle x \rangle = \frac{x_m s_n + x_n s_m}{s_m + s_n},$$
$$\langle s^2 \rangle = \frac{(m-1)s_m^2 + (n-1)s_n^2}{m+n-2},$$

where x is the value (δ_{aniso} or η) and s is the confidence interval of x for simulations of spectra obtained at two different spinning frequencies with m and n equal to the number of spinning sidebands used in each of the simulations.

A two-tailed F test was performed to confirm that the values for the two different spinning frequencies did not differ significantly from each other [20].

The principal values δ_{xx}, δ_{yy}, and δ_{zz} and their confidence intervals, $s_{\delta xx}$, $s_{\delta yy}$, and $s_{\delta zz}$, were calculated with the partial derivative method [21] using the values of δ_{aniso} and η at 95.4% confidence limit. The values for δ_{xx}, δ_{yy}, and δ_{zz} were then converted to δ_{11}, δ_{22}, and δ_{33}, according to the convention of Mason, $\delta_{11} > \delta_{22} > \delta_{33}$ [22].

The SIMPSON program [14] was used to calculate the ^{31}P spectra for the experimentally determined CSA parameters, using a CSA tensor to propagate an I_x density matrix, with the crystal file zcw376 and 19 γ angles. The spectral width, resolution and MAS rate were set to the values used experimentally.

The ^{207}Pb CSA parameters for the dtp complexes can not be simulated using the current version of the Mathematica program [13], because the values of δ_{aniso} are outside the current computational range of the program ($\delta_{\text{aniso}}\omega_0/\omega_r \leqslant 10$, where ω_0 is the Larmor frequency and ω_r is the spinning frequency). A rough estimate of the CST principal values from the spectra gives $|\delta_{\text{aniso}}| \approx 2000$ ppm. Therefore, a sample spinning frequency >15 kHz is required to enter the current computational range of the CSA simulation program. This high spinning frequency can not be reached in our MAS probe. Moreover, at such high spinning rates, the first rotational echo in the FID is largely distorted by the ring-down signal from the coil, which creates large phase and baseline distortions in the single-pulse ^{207}Pb NMR spectra.

However, the SIMPSON program [14] can be used to predict the ^{207}Pb CSA parameters. By looking at the sideband patterns in the experimental spectra an initial guess of the CSA parameters can be made, and further estimates and simulations can be performed until reasonable results are obtained.

3. Results and discussions

3.1. ^{31}P chemical shift anisotropy

Fig. 2 shows ^{31}P CP/MAS NMR spectra of three of the polycrystalline lead(II) dialkyldithiophosphate complexes: diethyl-, di-*iso*-propyl- and di-*iso*-butyl-, representing the three different types of molecular structures, i.e., mononuclear with van der Waals interactions between the monomers, polynuclear with covalent bonds between the monomers, and binuclear with one terminal and one tridentate ligand in each monomer, respectively, (recall Fig. 1).

These spectra, as well as the spectra of all the other lead(II) dtp complexes studied (see Table 2), display two resonance lines (94.4–100.0 ppm), flanked by spinning sidebands, which implies structural nonequivalence between the dtp ligands in these complexes. Note also the subsplitting of the resonance lines due to the two-bond $^2J(^{31}\text{P}–^{207}\text{Pb})$-couplings in some of the spectra (see Figs. 2A and B). These J-couplings will be discussed later in this article.

The shapes of the spinning sideband patterns are similar for all dtp ligands (except the more shielded resonance ($\delta_{\text{iso}} = 94.5$ ppm) in the di-*iso*-butyldithiophosphate complex), and are typical for the bridging ligands, or ligands with large S—P—S bond angles [12]. ^{31}P chemical shifts and ^{31}P CSA parameters for the complexes are given in Table 2. These data can be correlated with the known structural parameters of these compounds given in Table 1.

Fig. 3 shows the spectra obtained using the SIMPSON program [14] to calculate the spinning sideband pattern from the CSA data given by the spinning sideband analysis (Table 2). The sideband patterns are in excellent agreement with the experimental spectra (Fig. 2), and therefore, the ^{31}P CSA data given in Table 2 are reliable and can be further correlated to the known structural parameters of lead(II) dtp compounds given in Table 1.

All the lead(II) dialkyldithiophosphate complexes (see Table 2) have similar values of δ_{aniso} (in the range of −58 to −82 ppm). η varies between 0.2 and 0.9. There is only one exception: the more shielded phosphorus site in the di-*iso*-butyldithiophosphate lead(II) complex **5**

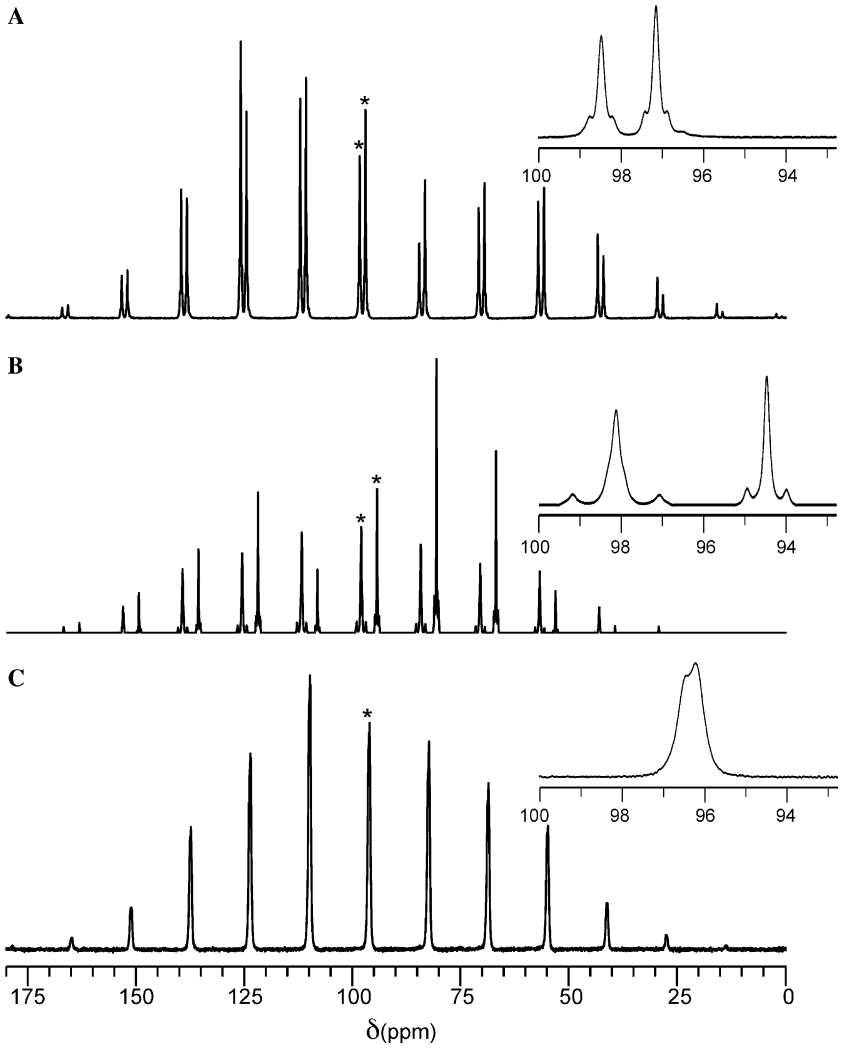

Fig. 2. ^{31}P CP/MAS NMR spectra of polycrystalline lead(II) diethyl- (A), di-*iso*-butyl- (B), di-*iso*-propyl- (C) dithiophosphate complexes. The spinning frequency was 2 kHz. Centrebands are marked by ∗. Insets show the central expanded region of the spectra.

has a positive value of δ_{aniso}, $\delta_{aniso} = 61.3$ ppm, $\eta = 0.38$. According to our previous results [12] the sign of δ_{aniso} depends on the S—P—S angle, which strongly affects the δ_{22} principal value of the ^{31}P chemical shift tensor. A plot of the principal components of the ^{31}P CST versus S—P—S bond angle (see Fig. 4A) shows that for the lead(II) dtp complexes in this study a change of sign of δ_{aniso} occurs in the region around 113°. The S—P—S angles in the lead(II) dtp complexes with known crystal structures are between 114° and 116° [7–11] (see Table 1). The only exception is the S—P—S angle of the purely terminal ligand in the di-*iso*-butyldithiophosphate complex **5**, which has an S—P—S angle of 112.0° [8]. This relatively small difference in comparison with the other lead(II) dtp complexes is enough to cause a change in sign of δ_{aniso}. It can also be seen from ^{31}P CSA data that η for the ligands with S—P—S angles close to 114° is close to 1, indicating a proximity to the "conversion point" where δ_{aniso} changes sign. Following the plot in Fig. 4A, the phosphorus sites with the largest δ_{22} values can be assigned to ligands with the largest S—P—S angles.

Similarly the phosphorus sites with the largest δ_{33} values can be assigned to ligands with the smallest S—P—S angles. The two S—P—S angles in lead(II) di-*cyclo*-hexyldithiophosphate are almost identical and the values of δ_{22} are the same to within their the confidence limits. In this case δ_{33} can be used to assign the ligands as this parameter differs significantly between the two phosphorus sites. Note that as δ_{22} and δ_{33} change simultaneously, but in opposite directions, the isotropic chemical shift is almost independent of the S—P—S angle, with a slight tendency towards larger shielding of the phosphorus sites with small S—P—S angles. Therefore, isotropic chemical shifts must be used with a certain degree of precaution in the assignment.

Fig. 4B shows a plot of the principal components of the ^{31}P CST versus the O—P—O angle. δ_{22} passes

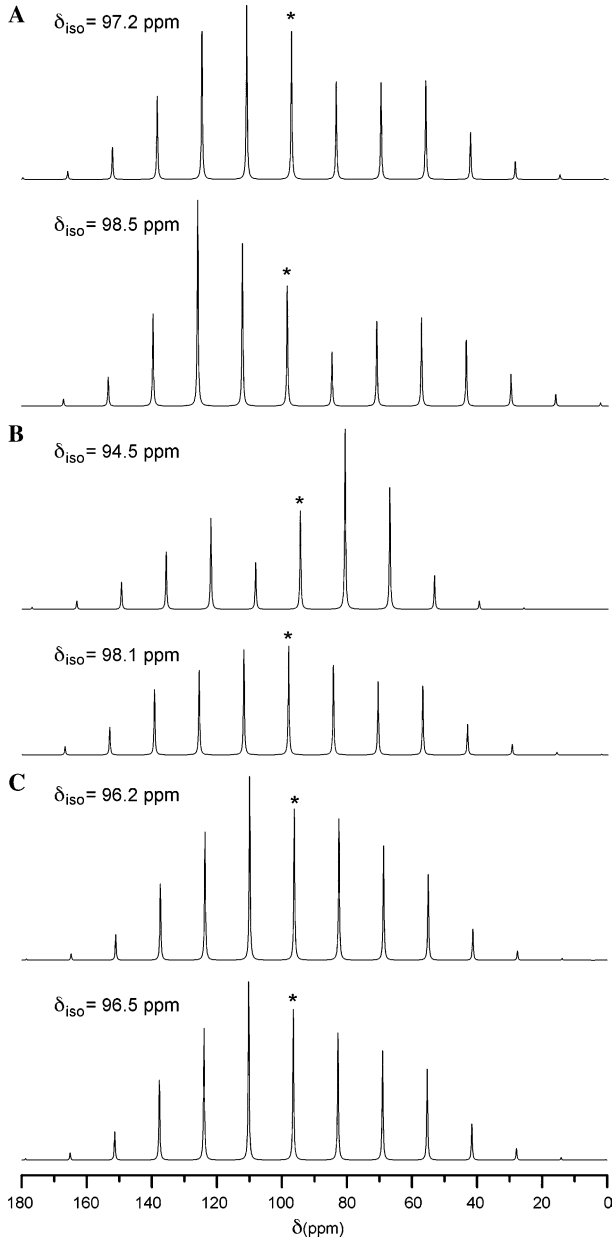

Fig. 3. ^{31}P MAS NMR spectra of different phosphorus sites in lead(II) diethyl- (A), di-*iso*-butyl- (B), di-*iso*-propyl- (C) dithiophosphate complexes as calculated by the SIMPSON program. The spinning frequency was 2 kHz. Centrebands are marked by *.

through a maximum at O—P—O ≈ 105° while δ_{33} passes through a minimum at the same value of the O—P—O bond angle. No noticeable correlations between S—P and O—P bond lengths and the principal values were found (see Figs. 4C and D).

We have previously reported the results of ab initio quantum mechanical calculations of the ^{31}P chemical shift tensor for a number of Ni(II) and Zn(II) dtp complexes, as well as calculations for a model fragment $[O_2PS_2]^-$ in which different structural parameters such as O—P and S—P bond lengths and O—P—O and S—P—S angles were varied (between 93° and 125°) [12]. The results showed that, in the relevant range, when the S—P—S angle increases δ_{22} also increases (^{31}P becomes less shielded), while δ_{33} decreases (^{31}P becomes more shielded). For increasing O—P—O bond angle δ_{33} increases, although this effect is less pronounced, and δ_{22} passes through a maximum at ca. 100° [12]. An increase in the S—P and O—P bond lengths will lead to a deshielding of the phosphorus sites [12]. However, experimental data on different dialkyldithiophosphate nickel(II) and zinc(II) complexes confirmed only the correlation between the S—P—S angle and δ_{22}, probably because of the relatively small variation in P—S and P—O bond lengths in these systems and the dominating effect of the S—P—S over the O—P—O bond angles on the principal values of the ^{31}P CST in these compounds [12].

The lead(II) dtp complexes follow the same trends as were found in our previously reported ab initio calculations on the model fragment $[O_2PS_2]^-$. For very small and very large S—P—S angles the ^{31}P chemical shift tensor adopts an almost axially symmetric shape ($\eta \to 0$), and is either oblate (positive δ_{aniso}, for small S—P—S angles) or prolate (negative δ_{aniso}, for large S—P—S angles). Fig. 5 shows the central fragment of a dialkyldithiophosphate lead(II) complex, with the principal axes frame of the ^{31}P CST given as in the $[O_2PS_2]^-$ model fragment [12]. δ_{33}, the axis corresponding to the smallest principal value, bisects the S—P—S angle, δ_{22} is perpendicular to the plane formed by the S—P—S atoms and δ_{11} is orthogonal to both δ_{22} and δ_{33}.

In our previous study of different potassium, nickel(II), and zinc(II) dialkyldithiophosphates [12], the S—P—S bond angles in the terminal ligands were in the range of 101° to 110° and in the bridging ligands these angles varied between 115° and 117°. For the lead(II) dtp complexes in this study the S—P—S angles are all between 112° and 116°. There is almost a linear dependence of the S—P—S angle on the ^{31}P CST principal value δ_{22} for the nickel(II), zinc(II) and lead(II) dtp complexes. However, the slopes of the lines between the data points of δ_{22} versus the S—P—S angle are different for the zinc(II), as compared with the lead(II) dtp complexes, (see Fig. 6). Note that δ_{22} is more sensitive to changes in the S—P—S angle in the lead(II) dtp complexes, as compared to the zinc(II) dtp complexes. For S—P—S angles larger than ~114° δ_{22}'s in the lead(II) dtp complexes are larger compared with δ_{22}'s in the zinc(II) complexes, whereas at small angles the opposite is true.

3.2. $^2J(^{31}P$–$^{207}Pb)$-coupling

Two-bond spin–spin couplings $^2J(^{31}P, ^{207}Pb)$ were observed in the NMR spectra of the two Pb(II) dtp complexes **1**, $[Pb\{S_2P(OC_2H_5)_2\}_2]$, and **5**, $[Pb\{S_2P(O\text{-}iso\text{-}C_4H_9)_2\}_4]$ (see Figs. 2A and B). Of the stable lead isotopes (^{206}Pb, ^{207}Pb, ^{208}Pb) only ^{207}Pb has $I \neq 0$ ($I = 1/2$, 22.1% n.a.), which gives rise to a splitting in the

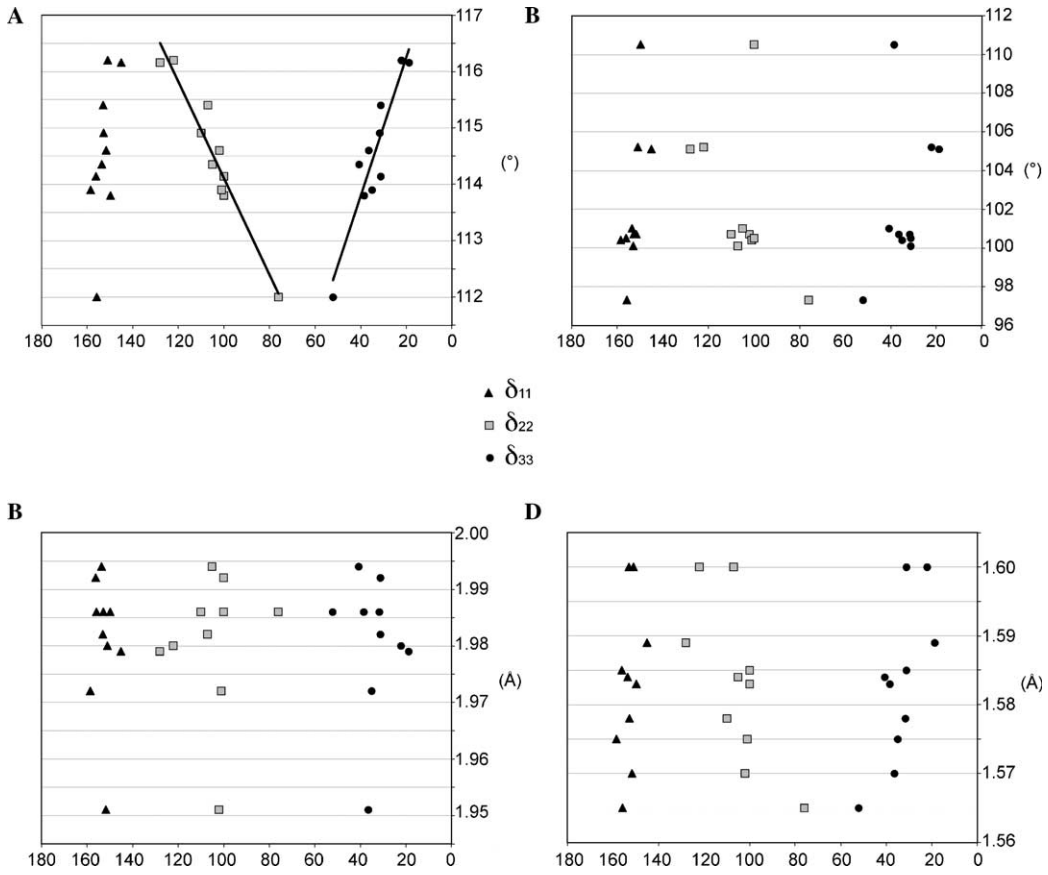

Fig. 4. Correlation between the chemical shift tensor principal values δ_{11}, δ_{22}, δ_{33}, and the S—P—S angle (A), the O—P—O angle (B), the S—P bond length (C), and the O—P bond length (D) in the dialkyldithiophosphate lead(II) complexes. The lines in (A) represent θ (°) $= 0.0847\delta_{22} + 105.65$ or δ_{22} (ppm) $= 11.806\theta - 1247.34$ ($R^2 = 0.931$) and θ (°) $= -0.1229\delta_{33} + 118.69$ or δ_{33} (ppm) $= -8.137\theta + 965.74$ ($R^2 = 0.8659$), respectively.

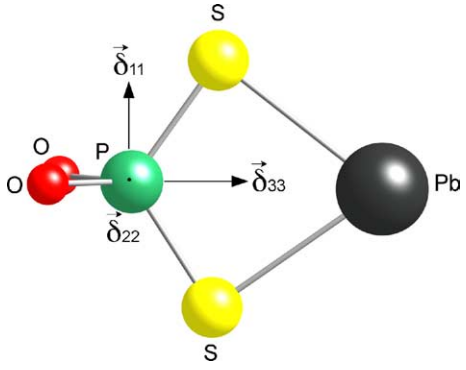

Fig. 5. Directions of the ^{31}P chemical shift tensor principal axes in the molecular fragment [O_2PS_2Pb].

^{31}P NMR spectra (two 'wing' lines in the three-line pattern, with relative intensities ca. 1:7:1). The phosphorus atom in each of the ligands is bonded to one lead atom through the terminal chelating P—S_2—Pb type of coordination. The two-bond *J*-coupling constants for the Pb(II) diethyldithiophosphate complex are ca. 80 Hz for each of the two non-equivalent P-sites. The outer doublet (1:1) is due to this *J*-coupling of phosphorus spins with one ^{207}Pb spin.

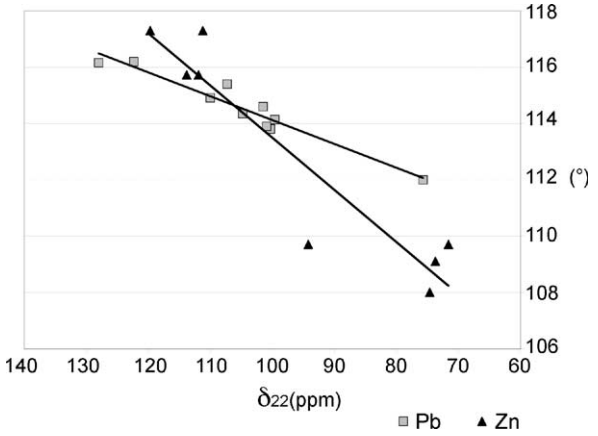

Fig. 6. δ_{22} versus the S—P—S angle for dialkyldithiophosphate zinc(II) and lead(II) complexes. The lines represent θ (°) $= 0.185\delta_{22} + 94.969$ or δ_{22} (ppm) $= 5.405\theta - 513.35$ ($R^2 = 0.881$), for the zinc complexes, and θ(°) $= 0.085\delta_{22} + 105.65$ or δ_{22} (ppm) $= 11.806\theta - 1247.34$ ($R^2 = 0.931$), for the lead complexes, respectively.

The ^{31}P NMR spectrum of lead(II) di-*iso*-butyldithiophosphate is more complex. The most shielded ^{31}P site with $\delta_{iso} = 94.5$ ppm, which we assigned to the terminal ligands because of the smaller S—P—S angle and posi-

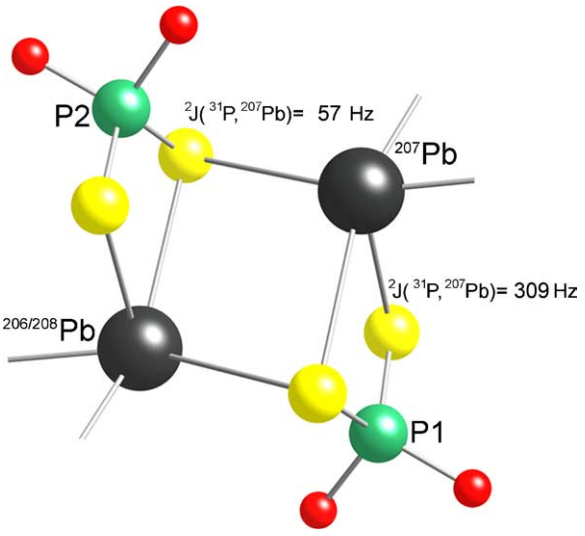

Fig. 7. The two P-atoms in the bridging ligands of the di-*iso*-butyldithiophosphate lead(II) complex are *J*-coupled to the two lead atoms in two different ways, either through terminal (P1) or bridging (P2) paths, leading to a double splitting in the ^{31}P NMR spectrum.

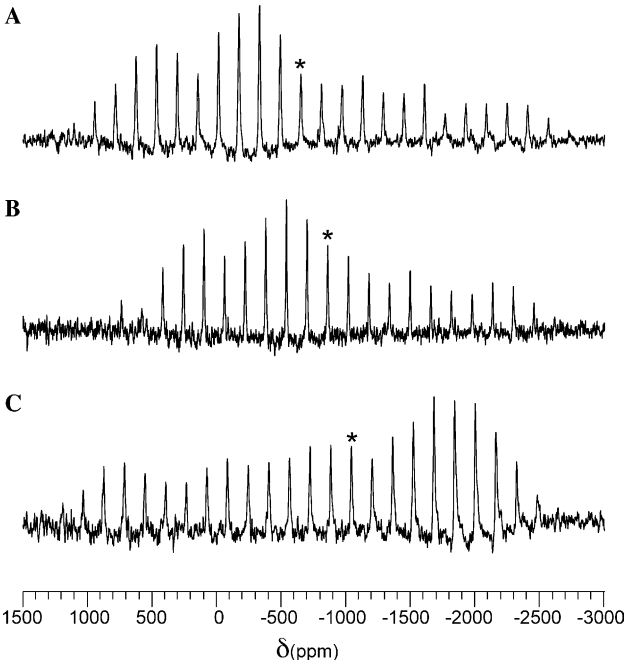

Fig. 8. ^{207}Pb MAS NMR spectra of polycrystalline di-*iso*-butyl (A), dipropyl (B), and diethyl (C) dithiophosphate lead(II) complexes. The MAS frequency was 12 kHz. Number of signal transients ca. 10,000–20,000. Centreband marked by ∗.

tive δ_{aniso} (see Table 2) shows a splitting of ca. 140 Hz (outer doublets). The least shielded ^{31}P site in this complex with $\delta_{iso} = 98.1$ ppm, which we assigned to the ligands with combined structural functions, shows a major splitting of ca. 309 Hz (outer doublets). However, each of these peaks is, in turn, additionally split with a *J*-coupling constant of ca. 57 Hz. This is an interesting case, seldomly seen in solid state NMR due to the lack of resolution. Therefore, we discuss it here in detail.

The central resonance line at 98.1 ppm stems from ^{31}P nuclei in isotopomers (molecules with different combination of different isotopes) with only non-magnetic lead isotopes (i.e., either ^{206}Pb or ^{208}Pb). This central line is split by ca. 309 Hz due to *J*-coupling between ^{31}P and ^{207}Pb ($I = 1/2$) within the terminal path of the complex (P1 in Fig. 7). The relative probability for such isotopomers is 22%, giving rise to a spectral pattern with intensity ratio 1:7:1. The central line is additionally split (ca. 57 Hz) by ^2J-coupling through the bridging path in the molecule (P2 in Fig. 7). The doublet ($J = 309$ Hz) is additionally split into a doublet by the presence of isotopomers in which both lead atoms are magnetic (^{207}Pb). Since the probability of having two ^{207}Pb-atoms within the same molecule is only ca. 5% the intensity of this subsplitting is small (1:7:1 in each satellite).

3.3. ^{207}Pb chemical shift anisotropy

Fig. 8 shows the ^{207}Pb spectra of three different dialkyldithiophosphate lead(II) complexes. The anisotropy is large and the general shapes of the spinning sideband patterns are similar for lead(II) dipropyldithiophosphate (Fig. 8B) and lead(II) di-*iso*-butyldithiophosphate (Fig. 8A), while the shape is different for the lead(II) diethyldithiophosphate (Fig. 8C). The *J*-coupling between ^{31}P and ^{207}Pb seen in the ^{31}P spectra of diethyl and di-*iso*-butyldithiophosphates can not be resolved in the ^{207}Pb spectra due to the large linewidths (ca. 750 Hz).

The ^{207}Pb chemical shifts for the three lead(II) dtp complexes are increasing when going from ethyl ($\delta_{iso} = -1040$ ppm) to propyl ($\delta_{iso} = -857$ ppm) and further to *iso*-butyl ($\delta_{iso} = -650$ ppm) ligands. Wrackmeyer has discussed that the ^{207}Pb chemical shifts depend on the coordination number of the lead atom in the complexes studied [23]. The higher the coordination number, the more shielded the lead site is. From the known X-ray structures the coordination numbers of lead in the dtp complexes given in Table 3 ($Pb[S_2P(OR)_2]_2$, R = C_2H_5, C_3H_7, *i*-C_4H_9) would be 4, 6, and 5, respectively. This can not explain the isotropic ^{207}Pb chemical shifts (see Table 3), as the lead(II) sites in the diethyldithiophosphate lead(II) complex would be most deshielded, and not most shielded according to the empirical rule of Wrackmeyer [23]. However, if the van der Waals bonds are considered as strong enough to contribute to the coordination sphere around the lead atom, the coordination numbers of Pb would be 8, 6, and 5, respectively. This hypothesis is currently under investigation and the results of theoretical DFT calculations will be reported elsewhere.

As mentioned earlier, CSA simulations with the Mathematica program could not be made for ^{207}Pb because δ_{aniso} was outside the computational limit of the

Table 3
^{207}Pb chemical shift tensor parameters for lead(II) dialkyldithiophosphates, as simulated by the SIMPSON program

Complex	δ_{iso} (ppm)[a]	δ_{aniso} (ppm)	η	δ_{11} (ppm)	δ_{22} (ppm)	δ_{33} (ppm)
$[Pb\{S_2P(OC_2H_5)_2\}_2]$	−1040	+2320	0.31	1280	−1840	−2560
$[Pb\{S_2P(OC_3H_7)_2\}_2]$	−857	−1900	0.60	663	−477	−2757
$[Pb\{S_2P(O\text{-}i\text{-}C_4H_9)_2\}_2]$	−650	−2020	0.60	966	−246	−2670

[a] Experimentally determined.

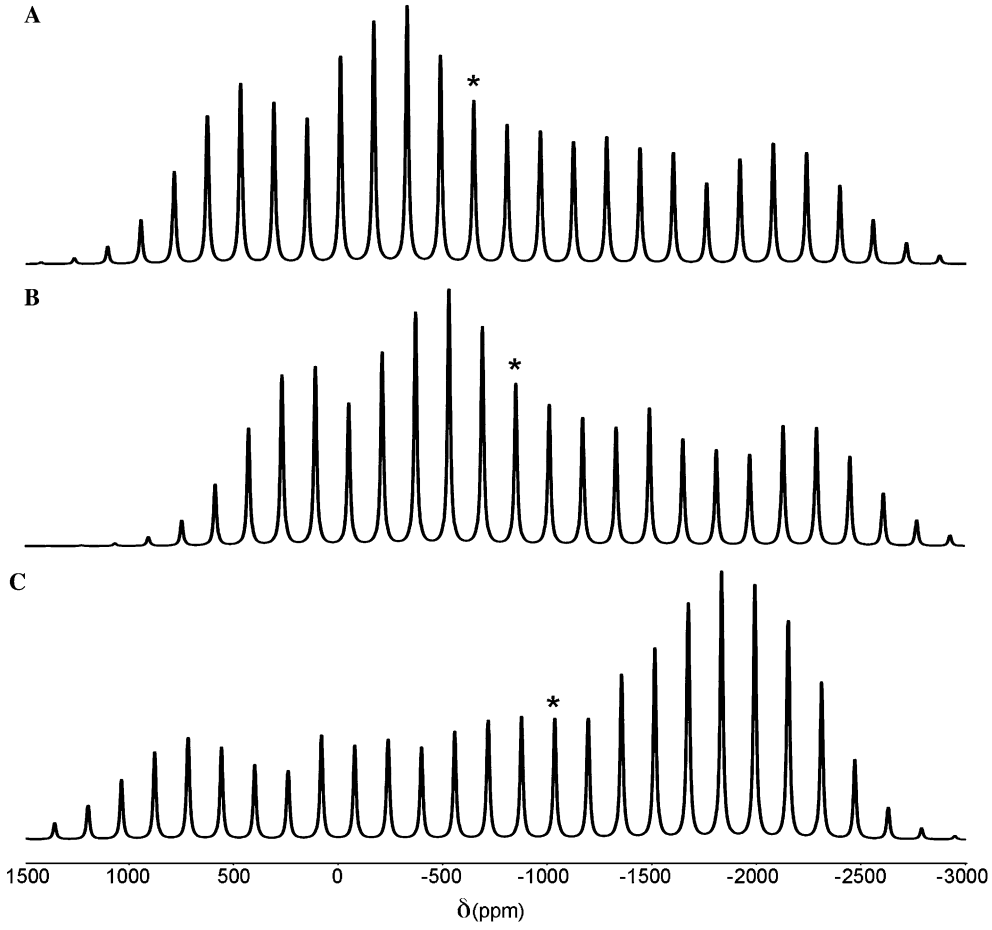

Fig. 9. ^{207}Pb MAS NMR spectra of di-*iso*-butyl- (A), dipropyl- (B), and diethyl- (C) dithiophosphate lead(II) complexes as simulated by the SIMPSON program. The MAS frequency was 12 kHz. Centrebands are marked by *.

program. Therefore, the SIMPSON program [14] was used to estimate the ^{207}Pb CSA parameters. The simulations were performed using a method similar to that described for the ^{31}P spectra. The CSA parameters were estimated using an iterative process, and correlate well with the experimental spectra. Fig. 9 shows the spectra given by the simulations using the SIMPSON program, and Table 3 gives the CSA parameters for these spectra.

The ^{207}Pb chemical shift tensor of the lead(II) diethyldithiophosphate complex has a more oblate form, as compared to the other two lead(II) dithiophosphates studied, whose tensors have a more prolate shape. The direction of the tensor within these complexes are not known, and therefore it is difficult to draw any conclusions regarding which structural factor(s) are causing this difference. However, a hypothesis can be suggested by looking at the coordination spheres around the lead. In all three cases the coordination spheres are distorted. The coordination sphere around Pb in diethyldithiophosphate is square-antiprismatic [8], with the lead atom located between the two square-planes, while the coordination sphere is pentagonal bipyramidal in propyl- [11] and square-based bipyramidal for *iso*-butyl- [8]. The fifth position in the pentagonal plane in the lead(II) dipropyldithiophosphate is occupied by a stereochemically active electron pair [11]. In lead(II) di-*iso*-butyldithiophosphate the stereochemically active lone pair occupies the top of one of the pyramids. In these two cases the

lead atom is located more or less in the plane. These differences in location of the lead atom should have an influence on the chemical shift tensor.

4. Conclusions

A number of polycrystalline *O*,*O*′-dialkyldithiophosphate lead(II) complexes were prepared and studied by solid-state ^{13}C, ^{31}P CP/MAS, and ^{207}Pb MAS NMR. ^{31}P isotropic chemical shifts revealed chemical and magnetic nonequivalence between the dialkyldithiophosphate ligands in the complexes, which is in accord with known crystal structures. Linear relationships between the S—P—S bond angle and the principal values δ_{22} and δ_{33} of the ^{31}P CST were established.

For two of the complexes, **1** and **5**, ^{2}J-couplings between ^{31}P and ^{207}Pb were resolved in the CP/MAS ^{31}P NMR spectra, which assists in the correct assignment of the resonance lines to phosphorus sites in either terminal ligands or in ligands with combined terminal and bridging functions.

^{207}Pb spectra were acquired in 20° single-pulse experiments with proton decoupling. ^{207}Pb CSA parameters for three lead dialkyldithiophosphates were estimated using the SIMPSON program.

Acknowledgments

We are grateful to CHEMINOVA AGRO A/S for the dialkyldithiophosphate chemicals that were kindly supplied for this study. The CMX-360 spectrometer was purchased with a grant from the Swedish Council for Planning and Coordination of Research (FRN) and part of the equipment was purchased with a grant from the foundation in the memory of J.C. and Seth M. Kempe. The work was also financed by Agricola Research Centre at Luleå University of Technology.

References

[1] J. Stary, The Solvent Extraction of Metal Complexes, Pergamon Press, New York, 1964.
[2] I. Haiduc, Thiophosphorus and related ligands in coordination, organometallic and supramolecular chemistry. A personal account, J. Organometall. Chem. 623 (2001) 29–42.
[3] J.F. McConnell, V. Kastalsky, The crystal structure of bis(diethyldithiophosphato)nickel(II), $Ni[(C_2H_5O)_2PS_2]_2$, Acta Cryst. 22 (1967) 853–859.
[4] A.V. Ivanov, A.-C. Larsson, N.A. Rodionova, A.V. Gerasimenko, O.N. Antzutkin, W. Forsling, Structural organization of nickel(II) and copper(II) *O*,*O*′-dialkyl phosphorodithioate complexes as probed by single-crystal X-ray diffraction, EPR, and CP/MAS ^{13}C and ^{31}P NMR, Russ. J. Inorg. Chem. 49 (3) (2004) 373–385, English translation.
[5] B.F. Hoskins, E.R.T. Tiekink, Structure of bis(*O*,*O*′-diisopropyl phosphorodithioato)nickel(II), $Ni[S_2P(O^iC_3H_7)_2]_2$, Acta Cryst. C 41 (1985) 322–324.
[6] A.J. Burn, G.W. Smith, The structure of basic zinc *O*,*O*-dialkyl phosphorodithioates, Chem. Commun. 17 (1965) 394–396.
[7] T. Ito, The crystal structure of metal diethyldithiophosphates. II. Lead diethyldithiophosphate, Acta Cryst. B 28 (1972) 1034–1040.
[8] Ph.G. Harrison, A. Steel, G. Pelizzi, C. Pelizzi, The influence of the remote organic group on the solid-state structures of lead(II) bis(*O*,*O*′-dialkyl)dithio-phosphates. The crystal and molecular structures of $Pb[S_2P(O\text{-}i\text{-}Bu)_2]_2$ and $Pb[S_2P(OPh)_2]_2$, Main Group Metal Chem. vol. XI (4) (1988) 181–204.
[9] S.L. Lawton, G.T. Kokotailo, Structure of lead(II) *O*,*O*-diisopropylphosphorodithioate, Nature 221 (1969) 550–551.
[10] S.L. Lawton, G.T. Kokotailo, The crystal and molecular structure of polymeric lead(II) *O*,*O*′-diisopropylphosphorodithioate, $Pb[(i\text{-}C_3H_7O)_2PS_2]_2$. Deformation of a hexathiocoordinate lead group by a stereochemically active lone pair of electrons, Inorg. Chem. 11 (2) (1972) 363–368.
[11] A.-C. Larsson, A.V. Ivanov, O.N. Antzutkin, A.V. Gerasimenko, W. Forsling, Complexation of lead(II) with *O*,*O*′-dialkyldithiophosphate ligands: ^{31}P and ^{13}C CP/MAS NMR and single-crystal X-ray diffraction studies, Inorg. Chim. Acta 357 (2004) 2510–2518.
[12] A.-C. Larsson, A.V. Ivanov, W. Forsling, O.N. Antzutkin, A.E. Abraham, A.C. DeDios, Correlations between ^{31}P chemical shift anisotropy and molecular structure in polycrystalline *O*,*O*′-dialkyldithiophosphate zinc(II) and nickel(II) complexes: ^{31}P CP/MAS NMR and ab initio quantum mechanical calculation studies, J. Am. Chem. Soc. 127 (7) (2005) 2218–2230.
[13] O.N. Antzutkin, Y.K. Lee, M.H. Levitt, ^{13}C and ^{15}N—chemical shift anisotropy of ampicillin and penicillin-V studied by 2D-PASS and CP/MAS NMR, J. Magn. Reson. 135 (1998) 144–155.
[14] M. Bak, J.T. Rasmussen, N.C. Nielsen, SIMPSON: a general simulation program for solid-state NMR spectroscopy, J. Magn. Reson. 147 (2000) 296–330.
[15] A. Pines, M.G. Gibby, J.S. Waugh, Proton-enhanced nuclear induction spectroscopy. A method for high resolution NMR of dilute spins in solids, J. Chem. Phys. 56 (1972) 1776–1777.
[16] K. Karaghiosoff, Phosphorus-31 NMR, in: D.M. Grant, R.K. Harris (Eds.), Encyclopedia of Nuclear Magnetic Resonance, Wiley, New York, 1996, pp. 3612–3618.
[17] W.L. Earl, D.L. VanderHart, Measurement of ^{13}C chemical shifts in solids, J. Magn. Reson. 48 (1) (1982) 35–54.
[18] G. Neue, C. Dybowski, M.L. Smith, M.A. Hepp, D.L. Perry, Determination of $^{207}Pb^{2+}$ chemical shift tensors from precise powder lineshape analysis, Solid State Nucl. Magn. Reson. 6 (1996) 241–250.
[19] W.H. Press, S.A. Teukolsky, W.T. Vetterling, B.P. Flannery, Numerical Recipes in C, (1994) 697.
[20] J.C. Miller, J.N. Miller, Statistics for Analytical Chemistry, third ed., Ellis Horwood PTR Prentice Hall, 1993, 60–62.
[21] J. Kragten, Calculating standard deviations and confidence intervals with a universally applicable spreadsheet technique, Analyst 119 (1994) 2161–2165.
[22] J. Mason, Conventions for the reporting of nuclear magnetic shielding (or shift) tensors suggested by participants in the NATO ARW on NMR shielding constants at the University of Maryland, College Park, July 1992, Solid State Nucl. Magn. Reson. 2 (1993) 285–288.
[23] B. Wrackmeyer, Germanium, tin and lead NMR, in: D.M. Grant, R.K. Harris (Eds.), Encyclopedia of Nuclear Magnetic Resonance, Wiley, New York, 1996, pp. 2206–2215.